ELSEVIER

1 December 1998

Optics Communications 157 (1998) 335–342

OPTICS COMMUNICATIONS

Full length article

Pulse shape measurements using differential optical gating of a picosecond free electron laser source with an unsynchronized femtosecond Ti:sapphire gate

C.W. Rella *, G.M.H. Knippels [1], D.V. Palanker, H.A. Schwettman

Stanford Picosecond Free Electron Laser Center, W.W. Hansen Experimental Physics Laboratory, Stanford University, Stanford, CA 94305-4085, USA

Received 7 July 1998; revised 14 September 1998; accepted 14 September 1998

Abstract

We have measured the temporal pulse shape of a mid-infrared free electron laser using a 60 fs Ti:sapphire pulse as an optical gate. By employing a differential technique to simultaneously measure the instantaneous infrared intensity and its time derivative, we have reconstructed the pulse shape with sub-ps resolution, despite jitter the order of 50 ps between the two lasers. The experiment has been performed with two different types of gating methods: sum-frequency generation, which provides an instantaneous gate, and photo-induced plasma absorption, which supplies a step function gate. Differential optical gating can be generalized to include other gating methods, such as the optical Kerr effect or saturable absorption, thus permitting detailed pulse shape studies on a variety of optical processes, especially in the far-infrared, where conventional pulse shape measurement methods are more difficult to implement.

PACS: 42.65.Re; 42.65.Ky; 78.55.Ap; 41.60.Cr
Keywords: Ultrafast; Optical gating; Sum-frequency generation; Photo-induced absorption

1. Introduction

The development of ultrafast lasers has led to important advances in methods for characterizing the temporal profile of short optical pulses. With state-of-the-art semiconductor detectors and electronics resolution the order of 10 ps can be achieved [2], while conventional streak cameras permit ps resolution [3]. To characterize pulses shorter than the detector response time, a nonlinear optical gating technique can be employed (for both linear and nonlinear methods, see Ref. [1]). For high peak power pulsed lasers, the most common and useful method is to use the laser pulse itself as the optical gate. Using frequency doubling or polarization rotation, one can measure the second or third order autocorrelation function, which provides a clean, unambiguous measurement of the optical pulse length. Advanced techniques based on these nonlinear optical effects, such as frequency resolved optical gating (FROG) [2], give additional information about the optical frequency and phase. In fact, SHG-FROG measurements [3] have

* Corresponding author. FOM-Institute AMOLF, Kruislaan 407, 1098 SJ Amsterdam, The Netherlands. Tel.: +31-20-6081351; Fax: +31-20-6684106; E-mail: rella@amolf.nl

[1] Current address: FOM-Institute for Plasma Physics Rijnhuizen, P.O. Box 1207, 3430 BE Nieuwegein, The Netherlands.

[2] For example, the Model #1002/6, from New Focus, which has a rise time of 6 ps.

[3] For example, the Hamamatsu C5680 streak camera has a time resolution of 2 ps.

0030-4018/98/$ - see front matter
PII: S0030-4018(98)00504-5

been made on the Stanford free electron laser (FEL), the same laser upon which the measurements described here have been performed.

In certain cases, however, autocorrelation methods are not practical, either because the peak optical power is too low or the appropriate nonlinear crystals are unavailable. In these instances, it is often possible to obtain pulse shape information by employing a cross correlation technique using ultrafast gate pulses from an external laser. These pulses can be used to measure the temporal structure of even weak optical sources with a resolution corresponding to the length of the gate pulse. In practice, difficulties in synchronization require that the data be collected in a single shot, with a detector element for every time bin [1]. For visible and near-IR sources, sum-frequency generation or polarization rotation can be used as the gating mechanism, and sensitive array detectors, such as CCD arrays, can then be employed.

In the far-IR and beyond ($\lambda > 20$ μm), no materials (with the notable exception of the second-harmonic generating crystal DAST [4]) have been developed which provide efficient sum frequency conversion. Two potential gating mechanisms are polarization rotation [5] and photo-induced reflectivity [6] or absorption. To perform a single shot cross correlation using either gating scheme, a far-IR array detector is required. For relatively bright sources, pyroelectric arrays can be used successfully. Arrays of more sensitive detectors, however, can be difficult or expensive to obtain.

In this paper we describe a simple method called differential optical gating (DOG), from which detailed optical pulse shape information can be obtained via optical gating with an unsynchronized pulsed laser. The essence of the DOG technique is to measure simultaneously the intensity of the source pulse and its time derivative. Using a two-point cross correlator (described below), one can obtain from each source and gate pulse pair, or shot, a measurement of the intensity and derivative at a given (albeit unknown) point in time. Many such measurements must be made to reconstruct an accurate picture of the intensity envelope of the source pulse. If the time jitter between the sources is larger than the source pulse length, and given sufficient accumulation time, one obtains a map of the derivative I' as a function of the intensity I, or

$$\frac{\mathrm{d}I}{\mathrm{d}t} = F(I). \tag{1}$$

One can obtain time information by integrating this equation directly, yielding

$$\int_{I_0}^{I_1} \frac{\mathrm{d}I}{F(I)} = \int_{t(I_0)}^{t(I_1)} \mathrm{d}t = t(I_1) - t(I_0). \tag{2}$$

It is clear from Eq. (2) that for unambiguous reconstruction, the function $F(I)$ cannot have any zeroes, and must be single valued within a given quadrant of (I, I') space. This presents problems for even a simple pulse shape, which always has a zero in the derivative at the pulse maximum. Thus, using Eq. (2), one can reconstruct the rising and the falling edges of the pulse separately, but some uncertainty exists in joining these two sections at the peak of the intensity curve. As will be discussed later, however, the details of the peak can be inferred with reasonable accuracy from other information obtained using the same method.

In situations when an instantaneous gating mechanism is unavailable or impractical, a step function gate (such as provided by photo-induced absorption) can be used with the DOG technique. In this case, the two-point cross correlator provides not the instantaneous intensity I and its time derivative, as above, but the *time-integral* of the intensity and *its* time derivative (i.e., the intensity I itself). If we define $J(t)$ as the time integral of the intensity $I(t)$,

$$J(t) = \int_{-\infty}^{t} \mathrm{d}t I(t), \tag{3}$$

then, by analogy to Eqs. (1) and (2), we find

$$\frac{\mathrm{d}J}{\mathrm{d}t} = G(J). \tag{4}$$

$$\int_{J_0}^{J_1} \frac{\mathrm{d}J}{G(J)} = \int_{t(J_0)}^{t(J_1)} \mathrm{d}t = t(J_1) - t(J_0). \tag{5}$$

Although mathematically identical to the equations governing the analysis of the instantaneous gate, it is important to note a few practical differences: (1) Because $I(t)$ is a positive function, the integral function $J(t)$ is therefore a positive and monotonically increasing function of time. Thus, all data collected exists in the first quadrant of a $\mathrm{d}J/\mathrm{d}t$ versus J graph. and the integral DOG method therefore does not suffer from the uncertainty in the vicinity of the pulse maximum. (2) Because of the integral nature of the gate, multiple pulses are easy to distinguish. Only the time between subpulses (when the intensity is essentially zero) cannot be measured with the integral DOG technique. (3) No practical gate is a true step function. The effect has a finite rise-time as well as a finite lifetime. Both time scales must be taken into account before reasonable results can be obtained. (4) To obtain the intensity profile as a function of time, $I(t)$, one must take an additional time derivative of the data. For raw data of similar quality, this leads to an reduction of the quality of the reconstructed pulse as compared with instantaneous DOG.

Differential optical gating is a simple method for measuring the shape of an optical pulse using an unsynchronized ultrafast laser. It can be used for the study of low intensity sources throughout a broad range of wavelengths. The DOG method is particularly useful in the far-infrared, where the lack of efficient nonlinear materials and high quality array detectors complicates the application of other techniques. One interesting candidate for study with the DOG method is coherent transition radiation from a parti-

cle beam [7]. Accurate measurement of the transition radiation temporal pulse shape provides a direct measurement of the temporal distribution of the particle beam. This information is of great technological importance to the design and operation of modern accelerators [8]. A second interesting candidate source to study using the DOG technique is the long wavelength (>20 μm) optical pulses generated by FELs such as FIREFLY [9] at Stanford University and FELIX [10] in the Netherlands. Measurement of the pulse shape would provide important information not only for FEL design but for the researchers who use these lasers in a variety of optical experiments.

Here we report DOG measurements on the mid-infrared FEL source at Stanford (for an overview of the operating parameters of the Stanford mid-infrared FEL, see Ref. [11]), using DOG with both an instantaneous gate (sum-frequency generation) as well as an integral gate (photo-induced absorption). We have chosen to make initial DOG measurements on this source so that comparisons can be made to conventional autocorrelations using second harmonic generation. This FEL produces infrared pulses tunable from 3–12 μm, with energies the order of 1 μJ. Each optical pulse (called a micropulse) is of picosecond duration, with a repetition rate of 11.8 MHz. A 60 fs Ti:sapphire laser (Tsunami, Spectra Physics, Santa Clara, CA, USA) tuned to 780 nm provides the gating pulse. The repetition rate of this laser is about 82.6 MHz, or the seventh harmonic of the FEL micropulse repetition rate. For the measurements described here, the two lasers were frequency (not phase) synchronized, such that the phase jitter between the two lasers was roughly 50 ps, which varied on a ms time scale. Removing this synchronization entirely and allowing the two lasers to free run would have increased the data acquisition time substantially, but would not have fundamentally changed the results.

We first present a detailed description of the measurements made using the instantaneous DOG technique. Following this are details of the pulse shape measurement made with the integral DOG method. The techniques are naturally very similar, so only the differences are highlighted before results are presented. In both cases, the DOG measurements are compared to simultaneous autocorrelation measurements to verify the validity of the technique. For all pulse shapes collected, the DOG pulse shapes were consistent with autocorrelations within measurement uncertainty.

2. Instantaneous differential optical gating (DOG)

For the instantaneous DOG experiments, a two-point cross-correlation apparatus was used to measure the intensity and derivative. The FEL was tuned to 6.3 μm, where the absence of strong atmospheric absorption insures that the optical pulse does not experience temporal distortion as it travels through the air. In this apparatus (depicted in Fig. 1), the source and gating beams are split into equal parts

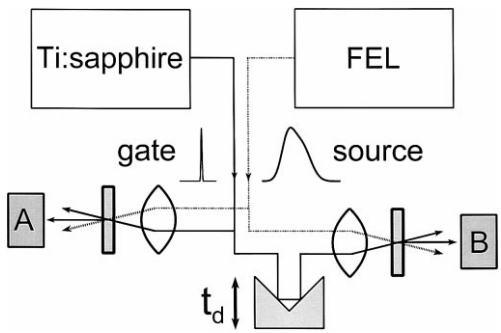

Fig. 1. Schematic of the two-point cross-correlator used to perform the DOG measurements. Depending on the gating material and mechanism, one may monitor either the transmitted source or gate beams, or another signal, such as is the case for sum-frequency generation.

and directed into two separate cross-correlators, or arms. In each arm, one source and one gate beam is focused and crossed in a nonlinear mixing crystal ($AgGaS_2$, Type-I phase matching) to produce photons at the sum frequency of source and gate. This signal is collected using silicon photodiodes. The two arms are identical with the exception of an optical delay line in one arm on the source beam which provides an additional small time delay t_d. We were careful to match the optics, detectors, and electronics in each arm to avoid unwanted artifacts.

The signal on each detector from each micropulse is given by a simple expression:

$$S(\Delta t) \propto \int_{-\infty}^{\infty} \mathrm{d}t' I_G(t') I_S(t' + \Delta t). \tag{6}$$

In this equation, I_G is the intensity envelope of the gating pulse, I_S is the envelope of the FEL pulse, and t is the difference in arrival time between the two pulses. Because the Ti:sapphire pulse is much shorter than the FEL pulse, $I_G(t')$ can be approximated by a delta function, and Eq. (3) reduces to

$$S(\Delta t) \propto E_G I_S(\Delta t), \tag{7}$$

in which E_G is the energy of the Ti:sapphire pulse. Thus from this expression one obtains a value for the intensity at a given point in time. The time derivative is not measured directly; instead, one approximates the derivative from the difference between two intensities spaced closely in time. The signal in each arm 'A' and 'B' is given by

$$I_S(t_J) \propto S_A(t_J)$$
$$I_S(t_J + t_d) \propto S_B(t_J + t_d), \tag{8}$$

where t_J is the difference in arrival time between the two pulses caused by jitter in the laser repetition frequencies, and t_d is the additional time delay on the FEL in arm 'B' of the apparatus. In Eq. (5), we have assumed that E_G is constant. Typically the energy fluctuations are less than 2% rms in our Ti:sapphire laser system. The magnitude of

the FEL intensity at a time $t_J + \frac{1}{2}t_d$ is proportional to the average of S_A and S_B, and the time derivative of the intensity averaged during this same region of time is given by the difference of S_A and S_B divided by t_d, or

$$\bar{I}'_S\left(t_J + \frac{1}{2}t_d\right) \equiv \frac{I_S(t_J + t_d) - I_S(t_J)}{t_d}$$

$$\propto \frac{S_B(t_J + t_d) - S_A(t_J)}{t_d}. \qquad (9)$$

The time delay t_d must be chosen carefully to provide a sufficiently large difference on the slowly varying parts while maintaining adequate temporal resolution on the quickly varying parts. For these experiments, a delay of 0.66 ps was used.

For each shot, the intensity and its derivative are collected and stored by a computerized data acquisition system. After collecting several thousand such shots, one obtains a density map in (I, I') space. If the measurement could be made without noise, a simple pulse would yield a single curve in this coordinate space. In reality, any intensity fluctuations, pulse shape fluctuations, or noise due to difference in response between the two arms causes the curve to acquire a finite width. This noise will not only mask smaller features of the profile, but can also affect the ultimate time resolution of the experiment. It is difficult to quantify the precise manner in which the intensity noise influences the reconstructed intensity profile, although the most significant effect of intensity noise is to hide the portions of the pulse shape where the finite difference represented by Eq. (9) is smaller than the noise (such as the wings of the pulse, or the peak). The exact effect of this noise clearly depends strongly on the nature of the noise and shape of the pulse, and will differ from experiment to experiment; for instance, noise which is proportional to intensity will have a different effect than fluctuations in the pulse shape, and a pulse which has both fast and slow features will be more challenging to measure than a relatively smooth pulse.

A typical density map of I' vs. I for an FEL pulse is shown in Fig. 2. These data were collected over a period of about 1 min, corresponding to about 2.5×10^4 shots. The function $F(I)$ is obtained from this density map by tracing a curve which follows the centroid of the density distribution, as displayed by the heavy line in Fig. 2. The width of this distribution is caused primarily by FEL intensity fluctuations, which were about 5–10% rms. The data in Fig. 2 exhibit a strong asymmetry about the I axis, indicating that the pulse is asymmetric in time. It was verified that when the delay is changed from t_d to $-t_d$, the function $F(I)$ is reflected about the I-axis.

Using the curve $F(I)$ plotted in Fig. 2, the pulse shape is trivially reconstructed using Eq. (2). The function $F(I)$

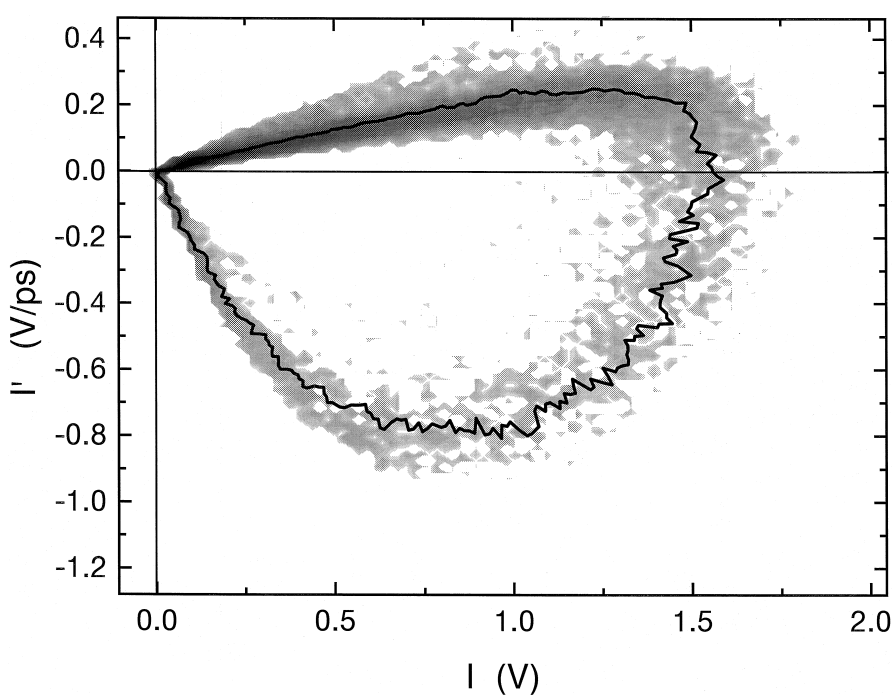

Fig. 2. Density map showing the log of the number of counts versus I and I'. Each count consists of a single measurement of I and I'. The vast majority of the counts occur where the derivative is small and positive, indicative of a slow rising edge and a fast trailing edge to the FEL pulse. The function $F(I)$ obtained using a simple centroid-finding algorithm is shown by the bold line in the figure.

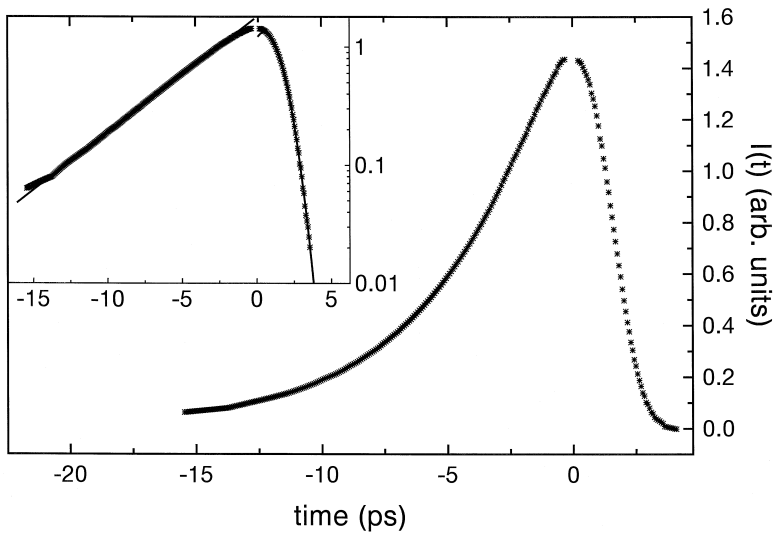

Fig. 3. The highly asymmetric FEL intensity envelope reconstructed from the raw data shown in Fig. 1. The main panel show the data on a linear scale. Note the small gap in the vicinity of the peak of the pulse; the width of this gap is inferred from the continuity of the density plot in the region $F(I) \approx 0$ and maximum I. The inset to the figure displays the same data in semi-log format. The rising edge is fit well by an exponential with a 4.45 ps time constant, while the trailing edge is fit well by a Gaussian with a width of 2.3 ps.

is double valued: for each intensity I, there exist two values for the derivative $F(I)$, corresponding to the rising and falling edges of the pulse. Each branch of $F(I)$ is integrated separately. To join the two regions, we take advantage of the fact that the density indicates the relative amount of time spent in a given part of the curve $F(I)$. If the timing jitter is large compared to the pulse width, one can compare the density in the peak region to the density on either side and thus infer the time duration of the peak. The resulting picture of the FEL pulse shape is shown in Fig. 3 on a linear scale. We emphasize that in reconstructing the pulse, a single-peaked FEL pulse was assumed; it is possible that more complicated FEL pulse shapes could produce data similar to that seen in Fig. 2.

The inset to Fig. 3 displays the same data in semi-log format, together with simple fits to the rising and falling edges of the pulse. The slow rising edge is fit well by a straight line, indicating an exponential dependence on time, whereas the falling edge is quadratic, which is indicative of a Gaussian. This shape is predicted [12] for the output of a low gain FEL oscillator with a relatively large cavity desynchronism [4] and high cavity Q; these data represent the first experimental verification of the theory. Further experimental investigation is underway to provide more rigorous tests of FEL theory than has been previously possible.

As a final check of the stability of the reconstruction process, the pulse shape shown in Fig. 3 is compared to data collected on a scanning second-harmonic intensity autocorrelator at the same time. Fig. 4 shows the measured autocorrelation data (circles) of the FEL beam together with the simulated autocorrelation obtained from the pulse shape obtained using the DOG technique. The data agree remarkably well, providing additional validity to the recon-

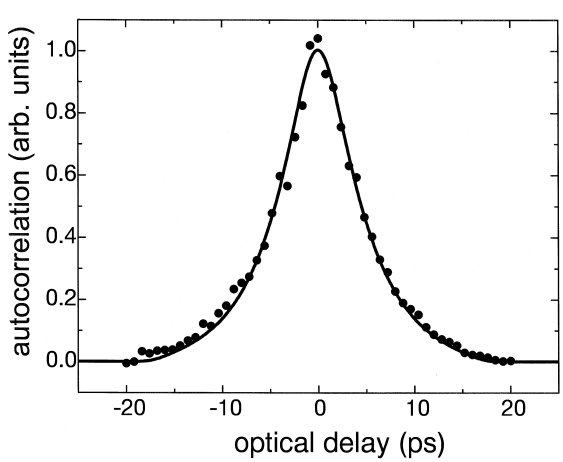

Fig. 4. Comparison of the simulated autocorrelation of the FEL pulse shape using DOG (solid line) with a conventional second-order autocorrelation of the FEL (circles). The two data sets were taken at essentially the same time. The raw autocorrelation data were rescaled vertically and offset by a few percent to match the two curves. No horizontal scaling was performed.

[4] Cavity desynchronism is the difference in length between the round-trip distance in the FEL oscillator and the spacing of the electron beam pulses; see, for example, Ref. [13].

struction process. Note that the DOG method provides a true intensity profile with sub-picosecond resolution, whereas the autocorrelation provides a *symmetrized* pulse shape.

As mentioned previously, even for simple pulse shapes, the analysis described above leads to uncertainty in the reconstruction where the derivative is zero. The fundamental principle behind the DOG technique is to correlate measured values of the intensity at a known time separation. However, one is not limited to small time delays. It is possible to eliminate the uncertainty at the peak by making an additional measurement at a larger time delay t_d the order of the pulse length. Thus, one can correlate the peak of the pulse to the wings where the differential analysis is valid. It may even be possible to eliminate the ambiguity caused by multiply peaked pulses by a similar set of measurements. A theoretical investigation is currently underway to answer this question. For the relatively simple FEL pulses measured here, however, the conceptually simple differential analysis is adequate.

3. Differential optical gating with an integrating gate

To test the integral DOG method, the FEL was tuned to 10 μm. The gating mechanism used in the test was photo-induced plasma absorption, a process by which above band-gap photons from the Ti:sapphire excite free carriers in a semiconductor, which in turn strongly absorb the incoming infrared radiation. The apparatus used to implement the integral DOG technique is nearly identical to that described above and shown in Fig. 1. Just two small changes were made. First, the $AgGaS_2$ crystals were replaced with thin (1 mm) slabs of infrared optical quality germanium, a common semiconductor transparent throughout the mid-infrared at 2 to 14 μm, and at wavelengths longer than 35 μm. Secondly, an infrared MCT (mercury cadmium telluride) detector was used to monitor the transmitted infrared power in each arm.

The near-infrared pulses from the Ti:sapphire oscillator are too weak to induce significant free carrier absorption in the semiconductor; therefore, the 1 mJ output pulses of a regenerative Ti:sapphire amplifier were used to pump the germanium slabs. Because of the limited (1 kHz) repetition rate of the Ti:sapphire amplifier, combined with the 3% duty factor of the FEL, the effective repetition rate was reduced to roughly 30 shots/s. However, the synchronization characteristics between the two lasers were unchanged from the instantaneous DOG experiment.

For times before the gating pulse arrives, the germanium is essentially transparent. However, for all times after the gate pulse arrives, the semiconductor becomes opaque to infrared radiation. Therefore, unlike the case of the instantaneous gate, where the shape of the gate is the intensity profile of the Ti:sapphire pulse, photo-induced plasma absorption provides a step-function gate. If we

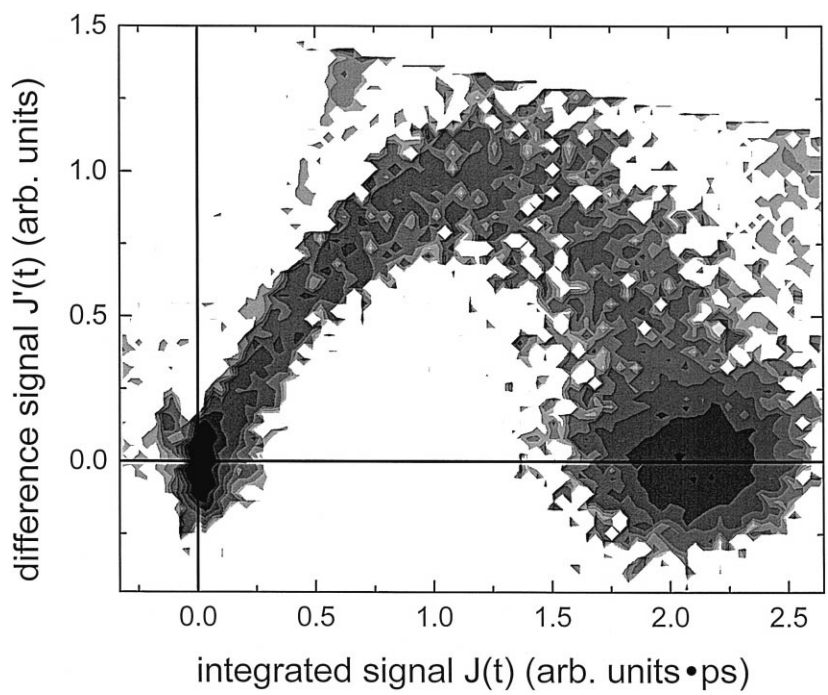

Fig. 5. Density map for the integral gating method, showing the log of the number of counts versus the gated signals J and J'. One count consists of a single measurement of J and J'. The function $G(I)$ (not shown here) is obtained using a centroid-finding algorithm.

again assume that the gating pulse is much shorter than the source pulse, and further that the carrier lifetime is infinite on the time scale of the problem, then the gate may be assumed to be an ideal step function. The expression for the transmitted signal as a function of time between the two pulses is

$$S(\Delta t) \propto \int_{-\infty}^{\Delta t} \mathrm{d}t' I_S(t'). \tag{10}$$

Note that the photo-induced absorption gate has the additional advantage that, provided the Ti:sapphire pulses have enough energy to saturate the effect, the characteristics of the gate are relatively insensitive to power fluctuations in the gating beam.

Eq. (10) is clearly just the time integral of the source intensity envelope, given by $J(t)$ in Eq. (3). The analysis proceed precisely as before, with the source intensity $I(\Delta t)$ replaced by $J(\Delta t)$. We thus arrive at the final form for the time derivative of $J(t)$ in terms of measured quantities:

$$\bar{J}'_S\left(t_J + \frac{1}{2}t_d\right) \equiv \frac{J_S(t_J + t_d) - J_S(t_J)}{t_d} \propto \frac{S_B(t_J + t_d) - S_A(t_J)}{t_d}. \tag{11}$$

As before, it is necessary to choose t_d such that it is small enough to provide adequate time resolution, while large enough such that the difference signal between the two arms is not swamped by noise. For these measurements, t_d was 1 ps.

Fig. 5 shows a typical plot of J versus J'. The quality of the data is somewhat poorer than the data shown in Fig. 2. One reason is that because of the reduced data collection rate, fewer shots were collected. A second cause is that the MCT detectors used for the measurement had significantly more noise than the detectors used to detect the sum frequency signal for the instantaneous DOG method. These additional sources of noise forced the use of a relatively long time delay t_d of 1 ps. The reconstruction method used to obtain $J(t)$ is identical to that described above. To ultimately obtain $I(t)$, the source intensity envelope, it is necessary to take the time derivative of $J(t)$ numerically. Note that there are no ambiguities at the peak of the pulse. Fig. 6 shows the result of this process. A low-pass filter with a time constant of 0.25 ps was used on the result to remove the high frequency noise generated by taking the derivative. A simulated autocorrelation is generated from the intensity profile shown in Fig. 6. When compared to a simultaneous autocorrelation (not shown), the two methods agree on the optical pulse length to within 5%, further demonstrating the validity of the integral DOG method.

The pulse envelope shown in Fig. 6 is almost 2 ps long, which is just a factor of two longer than the time delay t_d. The method of approximating the derivative as a finite difference (as in Eq. (11)) will cause distortions in the pulse shape when the time delay is the order of the pulse length. For a more accurate measurement, a more complete reconstruction algorithm must be developed.

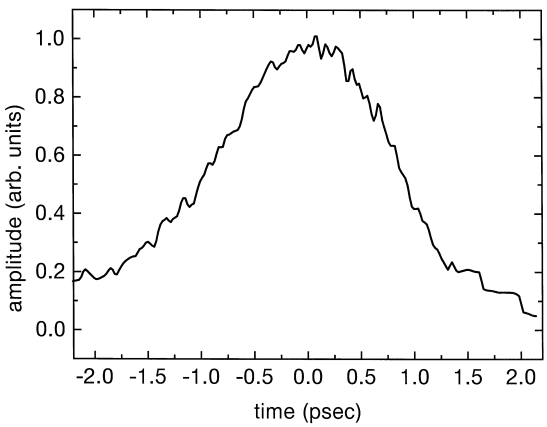

Fig. 6. Intensity profile of the FEL obtained at 10 μm using DOG with an integral gate, from analysis of the raw data depicted in Fig. 5. A low pass filter with a 0.25 ps time constant was used to remove the noise generated by taking the numerical derivative. Although a more nearly symmetric result, the pulse does exhibit a slight asymmetry, which is consistent with current FEL theory.

4. Conclusions

In conclusion, we have measured the pulse length of a mid-infrared FEL using DOG, with an unsynchronized fs Ti:sapphire laser providing the gating pulse. The pulse shape has been measured with sub-picosecond resolution, despite a jitter between the source and gating pulses of 50 ps. We have used two different gating mechanisms, one instantaneous and one which integrates in time. Each method has advantages. For simple pulse shapes, the instantaneous DOG technique provides extremely high quality pulse shape information, but more complex pulse shapes are difficult to measure. The integral DOG method, although the data is somewhat poorer, has the advantage that multiple pulses are easily resolved.

Because DOG can be performed throughout a broad wavelength regime, it provides a simple alternative to conventional pulse length measurement techniques, especially at long wavelengths. Promising applications include measurements of terahertz transition radiation from charged particle beams and long wavelength FELs.

Acknowledgements

We acknowledge the efforts of Todd Smith and the rest of the research group at the Stanford Picosecond FEL Center, and we thank Robert Laughlin of the Stanford

Physics Department for stimulating discussions. We also thank Roger Route of the Stanford Applied Physics Department for providing the $AgGaS_2$ crystals. This work has been supported by ONR contract #N00014-94-1024.

References

[1] J.C. Diels, W. Rudolph, Ultrashort Pulse Phenomena, Chap. 8, Academic Press, 1996, pp. 365–399.
[2] R. Trebino et al., Rev. Sci. Instr. 68 (1997) 3277.
[3] B.A. Richman et al., Opt. Lett. 22 (1997) 721.
[4] N.A. van Dantzig et al., Opt. Lett. 23 (1998) 466.
[5] R.L. Sutherland, Handbook of Nonlinear Optics, Marcel Dekker, New York, 1996, 295 pp.
[6] L. Zheng et al., Opt. Lett. 20 (1995) 407.
[7] J.D. Jackson, Classical Electrodynamics, 2nd ed., Wiley, New York, 1975, 685 pp.
[8] P. Kung et al., Phys. Rev. Lett. 73 (1994) 967.
[9] K.W. Berryman et al., Nucl. Instr. Meth. A 375 (1996) 632.
[10] D. Oepts et al., Infrared Phys. Technol. 36 (1995) 297.
[11] K.W. Berryman et al., Nucl. Instr. and Meth. A 358 (1995) 300.
[12] W.B. Colson, in: W.B. Colson, C. Pellegrini, A. Renieri (Eds.), Laser Handbook, Vol. 6, North-Holland Publishing, Amsterdam, 1990, p. 179.
[13] C.A. Brau, Free Electron Lasers, Academic Press, Boston, 1990, 22 pp.